DOI 10.1007/s11018-020-01759-3
Measurement Techniques, Vol. 63, No. 2, May, 2020

HIGH VOLTAGE MONITORING WITH A FIBER-OPTIC RECIRCULATION MEASURING SYSTEM

A. V. Polyakov[1] and M. A. Ksenofontov[2]

UDC 681.785:681.7.068

Optical technologies for measuring electrical quantities have unique properties and significant advantages in the high-voltage electric power industry; for example, the use of optical fibers ensures the high stability of measuring equipment to electromagnetic interference and galvanic isolation of high-voltage sensors; external electromagnetic fields do not influence the data transmitted from optical sensors via fiber-optic communication lines; problems associated with ground loops are avoided, and there are no side electromagnetic radiation or cross-coupling between the channels. The structure and operation principle of a quasi-distributed fiber-optic recirculation system for monitoring high voltages are presented. The sensitive element of the system is a combination of a piezoceramic tube with an optical fiber beam waveguide where the inverse transverse piezoelectric effect occurs. The electrical voltage measurement principle is based on recording the change in the recirculation frequency under the applied voltage influence. When the measuring sections are arranged in ascending order of the measured effective voltages relative to the receiving-transmitting unit, a relative resolution of 0.30–0.45% for the PZT-5H and 0.8–1.2% for the PZT-4 is achieved in the voltage range of 20–150 kV.

Keywords: *high voltage, fiber-optic measuring system, recirculation frequency, reverse transverse piezoelectric effect, resolution.*

Introduction. The accelerated development of automated control and management systems in all industrial fields has led to increasing demand for transducers (sensors) for measuring various physical quantities such as temperature, pressure, acceleration, displacement, and current strength. In addition to the good metrological characteristics of such sensors, they are characterized by high reliability, stability, noise immunity, durability, as well as ease of integration with microcontroller control systems. This is especially true for industries such as aviation electronics, metallurgy, auto electronics, heat engineering and energy engineering, medical technology, and high-precision weapons systems. An example of a sensor that meets the listed requirements is the fiber-optic sensor (FOS).

In modern energy-saturated industries, stringent requirements are imposed on the metrological parameters of electrical sensors. This often leads to the intractable problem of protecting the sensors from various electromagnetic interferences, which are especially significant when the sensors are far removed from the information accumulation platforms. Therefore, for electrical measurements in the energy sector, optical methods are increasingly considered as promising alternatives to electrical methods. Optical methods have several advantages over electrical methods, such as a wider frequency band and an extended dynamic range and good dielectric properties combined with high fire safety and corrosion resistance.

The FOSs of electric voltage are designed, in particular, for the remote control of parameters of HVPLs and transformer substations necessary for power supply to enterprises and settlements. According to their purpose and the current voltage value, HVPLs are divided into the following classes:

[1] Belarusian State University, Minsk, Republic of Belarus; e-mail: polyakov@bsu.by.
[2] Sevchenko Institute of Applied Physical Problems, Belarusian State University, Minsk, Republic of Belarus; e-mail: lab_dozator@mail.ru.

Translated from Izmeritel'naya Tekhnika, No. 2, pp. 38–44, February, 2020. Original article submitted October 9, 2019; accepted November 5, 2019.

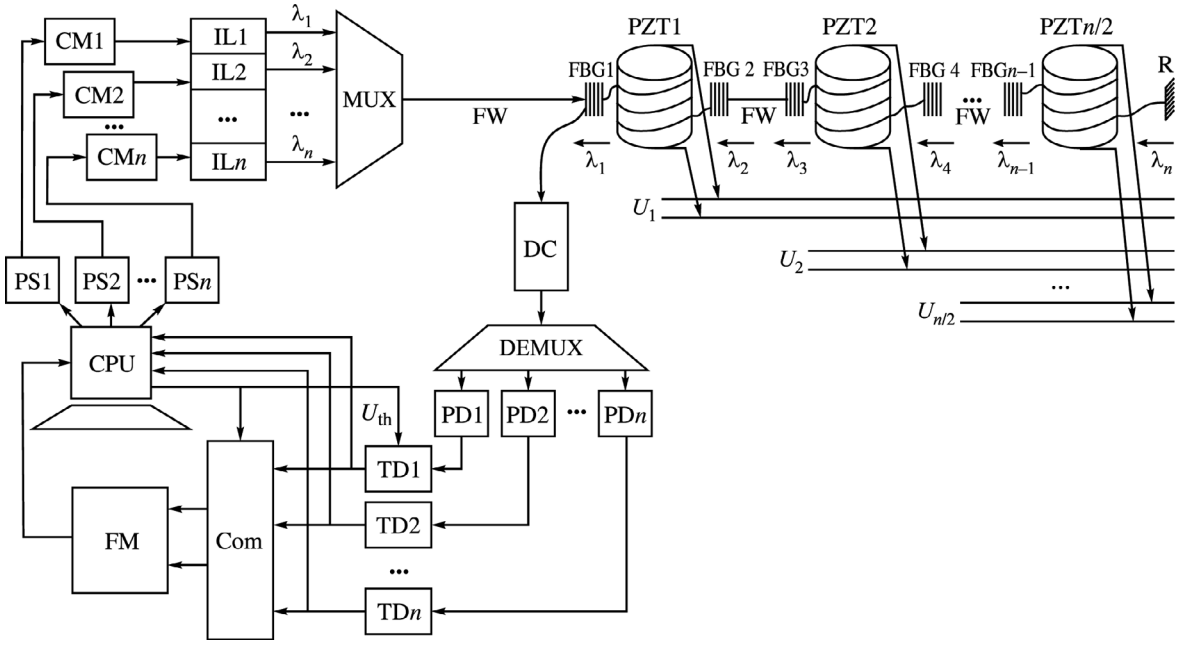

Fig. 1. Block diagram of a quasi-distributed fiber-optic high voltage measuring device: PS1–PSn – pulse shapers; CM1–CMn – current modulators; IL1–ILn – semiconductor injection laser set; MUX – multiplexer; FW – optical fiber beam waveguide; DC – directional coupler; DEMUX – demultiplexer; FBG1–FBGn – fiber Bragg gratings; PZT1–PZTn/2 – piezoceramic tubes; PD1–PDn – photodetectors; TD1–TDn – threshold devices; Com – commutator; FM – dual-channel frequency meter; R – reflector; CPU – control and processing unit.

– ultra-long high-voltage lines with a voltage of at least 500 kV for communication of individual power systems;

– 220 and 330 kV high-voltage trunk lines for transferring energy from powerful power plants, as well as for connecting power systems and combining power plants within power systems, for example, for connecting a power plant to distribution points;

– distribution high-voltage lines with voltages of 35, 110, and 150 kV for power supply to enterprises and settlements of large regions;

– high-voltage lines of not more than 20 kV for supplying electricity to consumers.

The latter two classes of HVPLs are most prevalent and are therefore of practical interest.

Several types of optical voltage sensors have been developed using the electro-optical Pockels effect (optical information is transmitted through the optical fiber) and macrostrains of the optical fiber, sensors with various constructive combinations of optical fibers and piezoelectric materials based on the Michelson interferometer, and sensors based on optical fiber Bragg gratings [1–8]. However, factors related to interferometric measurement methods affect the stable operation of such sensors, and they are as follows: measurement error arising due to the relative change in the arm lengths of the interferometer under fluctuations in temperature and pressure; the need for constant monitoring of the polarization of radiation to reduce the associated attenuation; and high sensitivity of the interference pattern to vibrations and other mechanical influences. The resolution of meters based on fiber Bragg gratings is limited by the width of their spectral reflection line and the resolution of the optical spectrum analyzer. All the above determine the relevance of developing new methods for recording and processing optical signals and constructing fiber-optic high voltage measuring systems that combine the basic principles of reliability and low cost with multifunctionality and high accuracy of measurements.

A fiber-optic recirculation system for measuring electrical voltage. Improving the operational characteristics of the FOS is associated with the use of the frequency measurement method. To control the voltage, using a quasi-distributed fiber-optic voltage sensor is proposed, and the operation principle of the sensor is based on recording changes in the recirculation frequency of a single pulse at individual wavelengths (Fig. 1). The electrical voltage is measured based on the sequential monitoring of changes in the difference in recirculation frequencies in neighboring sections at different wavelengths:

$$\Delta f_i(U) = f_{i-1}(\lambda_{i-1}) - f(\lambda_i).$$

A change in the recirculation frequency can be recorded with high accuracy with relative long-term instability of the recirculation frequency in the range of $(2–6)\cdot10^{-6}$ (depending on the length of the fiber beam waveguide FW) at a measurement time of 1 s [9, 10]. The sensitive element is a piezoceramic tube on which a fiber light guide is wound and rigidly fixed. In this device, an inverse transverse piezoelectric effect occurs; that is, the voltage applied to the tube leads to a change in its size, which entails a change in the length and refractive index of the fiber beam waveguide, and therefore the recirculation frequency. As a result of radial mechanical stresses under the influence of the applied voltage U, the change in the tube radius Δr is determined as follows [11]:

$$\Delta r/r = 2d_{31}U/h,$$

where d_{31} is the piezoelectric constant, and h is the tube thickness.

The emission sources are LDI-λ-DFB-2.5G-20/60 semiconductor injection lasers (Laserscom, Belarus), which are InGaAsP quantum well-based laser diodes with distributed feedback, assembled with an optical fiber in a sealed enclosure and covering the entire coarse wavelength division multiplexing range of radiation wavelengths 1270–1590 nm at a pitch of 20 nm. This enables the formation of up to eight measuring sections. The width of the emission spectrum in the continuous mode is 0.09 nm at an output power of 20 mW, and the peak power is 10 mW at a pump current $I = 50$ mA. The temperature coefficient of the change in wavelength is 0.1 nm/°C. Radiations at different wavelengths are combined by a multiplexer and directed through a fiber waveguide to sensitive elements–piezoceramic tubes. Piezoceramic materials are used as piezoelectric elements, which are represented by polycrystalline ferroelectric solid solutions. After synthesis, they are subjected to polarization in a constant electric field. Piezoceramics have a strong piezoelectric effect, high stability, high mechanical strength and resistance to external influences, comparative simplicity, and low manufacturing cost.

The diameter d of the tube was selected according to the following conditions: The minimum permissible bending radius of a single-mode fiber beam waveguide was determined based on the mechanical properties of the fiber. If the fiber is bent so much that surface stresses exceed 0.2%, it is very likely that cracks will occur in the fiber during operation. To prevent this, the following condition must be met:

$$d > 500D - 2h_1.$$

Here, the diameter of the fiber-optic sheath $D = 125$ μm, and the thickness of the protective coating layer $h_1 = 62.5$ μm (the outer diameter of the optical fiber with a polymer coating is 250 μm); that is, $d > 6.2$ cm ($r > 3.1$ cm). For PZT-4D-type piezoceramics based on titanium and lead zirconate (Morgan Matroc, UK), the maximum electric field strength $E = 14.4$ kV/cm; therefore, to measure voltages, for example, up to 20 kV, the tube thickness must be at least 1.5 cm.

The most common PZT-4D piezoceramic has a constant $d_{31} = 1.35\cdot10^{-10}$ m/V. This type of piezoceramic tube is selected due to its linear characteristic in a wide range of measured voltages and the absence of a hysteresis loop. The constant d_{31} is $2.74\cdot10^{-10}$ and $3.8\cdot10^{-10}$ m/V for piezoceramics PZT-5H (Morgan Matroc, UK) and PKR-73 (Research Institute of Physics, Southern Federal University, Rostov-on-Don, Russia), respectively. However, these materials belong to soft ferroelectric materials and feature hysteresis, which has to be considered, and the measured data must be corrected during processing.

Spectral radiation is selected using fiber Bragg gratings with a different period. Each grating is tuned to reflect a wave of a certain length $\lambda_1, \lambda_2, \ldots, \lambda_n$. The reflected signals pass through a directed coupler, are separated spatially in an optical demultiplexer, and then enter the photodetectors. The photodetectors are fast-acting InGaAs avalanche photodiodes Mitsubishi PD893D2 (Mitsubishi, Japan) with a spectral band of 1000–1600 nm, avalanche multiplication factor $M = 10$, load resistance $R_l = 50$ Ω, wavelength $\lambda = 1300$ nm, frequency band of 2.5 GHz, and sensitivity $S_\lambda = 0.85$ A/W at $M = 1$. Avalanche photodiodes do not require the use of electronic amplifiers at their outputs and enable to provide the necessary signal level. The electrical output signals of avalanche photodiodes are fed to threshold devices with an adjustable threshold of operation; these devices include an Am685 comparator (AMD, USA) and an F100125 level converter (Texas Instruments, USA). The threshold level of each device is individually set by the control and processing unit (CPU) so that, on the one hand, noise triggering is avoided (minimizing the likelihood of a false alarm), and on the other hand, the device operates steadily according to the useful signal level (minimizing the probability of signal omission). Threshold devices produce signals standard in

amplitude and duration that are fed to the pulse shapers (PS) through the CPU. Here electric pulses of the required amplitude, shape, and duration are formed. They are amplified by the current modulators (CM) and are pump current pulses for semiconductor radiation sources. Thus, the recycle closes. The measuring system also includes a two-channel frequency meter that records the recirculation frequency at each wavelength. The change in the difference of these frequencies according to the corresponding algorithm is converted into the voltage measured, which is recorded and displayed on the CPU monitor.

The principle of the meter operation is as follows: Lets, for example, injection lasers IL1 and IL2 generate radiation pulses at wavelengths λ_1 and λ_2, respectively. Impulses at wavelengths λ_1 and λ_2 are reflected from the gratings FBG1 and FBG2, respectively. The delay of the second pulse relative to the first is determined by the doubled length of the first fiber-optic section wound on the first piezoceramic tube PZT1. These pulses are detected by PD1 and PD2 photodetectors and enter the threshold devices TD1 and TD2, respectively, designed to avoid false alarms by noise pulses. Using a frequency meter, the recirculation frequencies at these two wavelengths are measured. The CPU contains a tunable electronic delay line necessary for processing data in each recycle. The pulse shapers set the required pulse duration, which will circulate in the system. A two-channel digital frequency meter measures for 1 s the recirculation frequencies of the first f_1 and second f_2 pulses at wavelengths λ_1 and λ_2, respectively. The difference between these frequencies $\Delta f = f_1 - f_2$ is calculated in the CPU. The deviation δf of the difference Δf due to a change in the optical fiber length under the influence of the applied voltage is the object of measurements. To monitor the voltage in another electrical device source (HVPL or substation transformer), using the commutator Com, for the corresponding fiber section, another pair of circulating signals at wavelengths λ_{i-1}, λ_i is selected. The length of each fiber-optic section is determined by the thickness of the piezoceramic tube, provided that the optical fiber is tightly wound in one row.

Modeling the resolution of the measuring system. One of the main metrological characteristics of the measuring system is the measurement error, which is determined, as a rule, during the metrological certification of a particular device. Since theoretical estimates are made in this article, it is more correct to consider one component of the total error, the error of the measurement method (MM). This error is associated with the resolution capability of the meter, and the smaller the error, the higher the resolution capability. The sensor resolution capability, i.e., the minimum change in the measured physical quantity, which can be unambiguously and reliably recorded, depends largely on the recirculation frequency instability. The recirculation frequency is described by the equation

$$f = [T_\mathrm{d} + 2Ln_e/c]^{-1},$$

where L is the length of the optical fiber beam waveguide section; $n_e = 1.467$ is the effective group refractive index of the fiber core; and T_d is the time delay of the pulse propagation in other elements of the circuit (injection laser, avalanche photodiode, other optoelectronic elements, and electronic units).

It is fluctuations T_d that determine the instability of the recirculation frequency f. The most significant influence on its change is exerted by the following factors: time jitter in the injection laser arising due to random changes in the delay time between the pump current pulse and laser radiation; instability of the avalanche photodiode response time; and time scatter of the threshold device triggering times, which is due to a change in the amplitude of the input signal and fluctuations of the triggering threshold.

The error of the MM of a fiber-optic recirculation sensor of electrical voltage is determined by the following condition: the relative change in the recirculation frequency when exposed to the optical fiber should exceed the maximum relative long-term instability χ_max of the recirculation frequency for the selected fiber length. The χ_max is due to the influence of external and internal destabilizing factors not related to the physical quantity measured. Thus, the following equation must be met:

$$\Delta f/f_0 = (f_0 - f)/f_0 = 1 - f/f_0 \geq \chi_\mathrm{max}, \tag{1}$$

where f_0 is the initial recirculation frequency.

The frequencies f_0, f and the periods T_0, T of recirculation are related by the following relationships:

$$f_0 = T_0^{-1}; \quad f = T^{-1}.$$

Then, Eq. (1) takes the form

$$1 - T_0/T = (T - T_0)/T \geq \chi_\mathrm{max}. \tag{2}$$

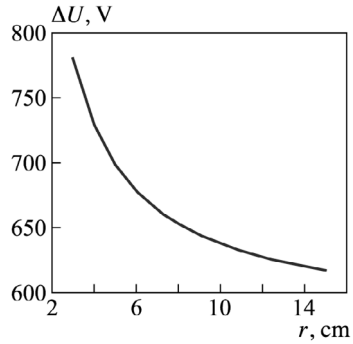

Fig. 2. Dependence of the error ΔU of the measurement method on the radius r of the piezoceramic tube for the fifth measuring section.

Assuming that the same voltage is applied to all piezoceramic tubes, the recirculation period of the ith section is described by the equation

$$T_0 = [2L_0 n_e + 2n_e \xi\gamma \cdot 2\pi rNi]/c = [2L_0 n_e + 2n_e \xi\gamma \cdot 2\pi rhi/d_f]/c, \quad (3)$$

where L_0 is the length of the undeformed fiber; ξ is the coefficient considering the effect of photoelasticity in the stretched part of the fiber (for quartz fibers, $\xi = 0.78$); γ is the coupling coefficient characterizing the degree of transmission of the tube deformation to the fiber (when they are rigidly coupled, $\gamma \approx 0.8$–0.9); N is the number of turns of fiber under the condition of winding in one row over the entire tube thickness; r and h are the radius and thickness of the tube, respectively; i is the number of the measuring tube; $d_f = 250$ μm is the fiber diameter.

Let the voltage in the ith section change to ΔU; then, the recirculation period of the ith measuring tube is expressed by the equation

$$T = [2L_0 n_e + 2n_e \xi\gamma \cdot 2\pi rh(i-1)/d_f + 2n_e \xi\gamma \cdot 2\pi(r + \Delta r)h/d_f]/c. \quad (4)$$

Taking into account Eqs. (3) and (4), the resulting difference in recirculation periods is as follows:

$$\Delta T = T - T_0 = 4\pi n_e \xi\gamma \Delta rh/(d_f c). \quad (5)$$

We use Eq. (5) in Eq. (2) and obtain

$$\frac{\Delta T}{T} = \frac{2\pi n_e \xi\gamma h\Delta r / d_f}{L_0 n_e + 2\pi n_e \xi\gamma hr(i-1)/d_f + 2\pi n_e \xi\gamma h(r+\Delta r)/d_f} = \chi_{max}. \quad (6)$$

From Eq. (6) we obtain

$$\Delta r = \frac{\chi_{max}(L_0 d_f + 2\pi\xi\gamma irh)}{2\pi\xi\gamma h(1-\chi_{max})}. \quad (7)$$

Using the equality $\Delta r = 2d_{31}\Delta Ur/h$ from Eq. (7), we obtain the resolution capability of the measuring system:

$$\Delta U_{min} = \frac{\chi_{max}(L_0 d_f + 2\pi\xi\gamma irh)}{4\pi\xi\gamma(1-\chi_{max})d_{31} r}. \quad (8)$$

Let us consider the variant of a consumer substation where the voltage must be controlled, for example, that of five lines with a voltage of 20 kV. We calculate ΔU_{min} according to Eq. (8) for $i = 5$, with a change in the radius r of the piezoceramic tube in the range of 3–15 cm and at $L_0 = 20$ m and $d_f = 250$ μm. Thus, continuous monitoring of the following conditions is required:

$$\text{if } 2(L_0 + 2\pi irh/d_f) < 100 \text{ m}, \text{ then } \chi_{max} = 5\cdot 10^{-6}; \quad (9)$$

$$\text{if } 2(L_0 + 2\pi irh/d_f) \geq 100 \text{ m}, \text{ then } \chi_{max} = 2\cdot 10^{-6}. \quad (10)$$

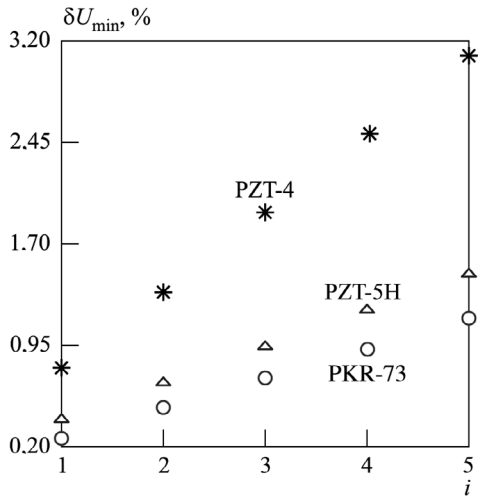

Fig. 3. Dependences of the relative resolution capability δU of a quasi-distributed sensor on the number i of the measuring sections when using piezoceramic tubes of different materials.

The results of calculations by Eq. (8) considering Eqs. (9) and (10) are presented in Fig. 2. The minimum error is registered for tubes of radius $r \le 12$ cm. With a further increase in the transverse dimensions of the tube, the relationships between the weight and size parameters of the tubes, their cost (manufacturing technology), and resolution capability will no more be significant.

By numerical simulation, we obtained the dependences of the change in the recirculation frequency on the measured voltage for PZT-4 ceramic tubes of different radii. These dependences can be approximated as a straight line represented as $\delta f = bU$, where b is the sensor sensitivity. As noted above, the sensitivity of the fiber-optic voltage sensor is increased for piezoceramic tubes with radii up to 12–15 cm; a further increase in the radii of the tubes does not improve the sensor metrological characteristics, while its sensitivity reaches 4.5 Hz/kV.

It follows from Eq. (8) that with an increase in the number of the measured HVPLs (i.e., with an increase in the total fiber length), the MM error increases. Let us consider the radius of the piezoceramic tube $r = 12$ cm (in accordance with Fig. 2) and calculate the voltage error of the MM for each controlled section $i = 1, ..., 5$ (Fig. 3) at $U_{max} = 20$ kW for tubes of various types. Figure 3 shows that if for the measurement points spaced at a large distance and one fiber-optic beam waveguide is used as the information line, the error can increase by 3.5–3.8 times. If five separate beam waveguides are used for measuring points located in approximately the same place, then the relative resolution capability the δU_{min} of each tube section will not exceed 0.8% for PZT-4 and 0.3% for PZT-5H and PKR-73.

In practice, there are often cases when several high-voltage lines with different voltages have to be controlled simultaneously. Let us consider the monitoring variant at the distribution station, where there are HVPLs of various voltages: $U_1 = 20$ kV, $U_2 = 35$ kV, $U_3 = 50$ kV, $U_4 = 110$ kV, and $U_5 = 150$ kV. In this case, Eq. (8) becomes

$$\Delta U_{min} = \frac{\chi_{max}(Ld_f + 2\pi\xi\gamma r_i h_i)}{4\pi\xi\gamma(1-\chi_{max})d_{31}r_i},$$

where

$$L = L_0 + \sum_{j=0}^{i-1} 2\pi\left(r_j + 2d_{31}U_j\frac{r_j}{h_j}\right)\frac{h_j}{d_f}. \qquad (11)$$

Thus, the tubes should be of different thicknesses: $h_1 = 1.5$ cm, $h_2 = 2.4$ cm, $h_3 = 3.5$ cm, $h_4 = 7.6$ cm, and $h_5 = 10.4$ cm. Fulfilling Eqs. (9) and (10) is still necessary, where the r and h should be substituted with r_i and h_i.

Since, according to Eq. (11), the error increases with an increase in the total beam waveguide length, to reduce the error, it is reasonable to use fiber beam waveguides of the same length equal to, for example, the length of the fiber for winding the tube of the smallest height for winding each piezoceramic tube. In this case, Eq. (11) becomes

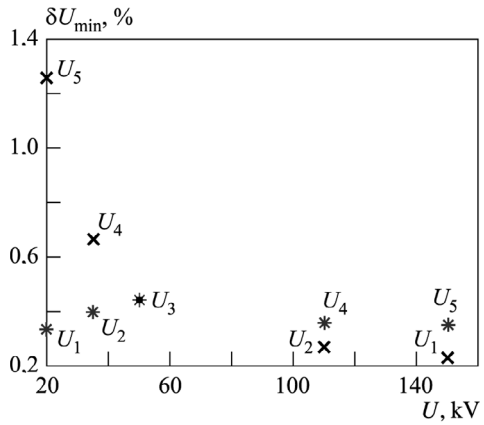

Fig. 4. Dependences of the relative resolution capability on the voltage measured with the arrangement of sensing elements in ascending order U_1 = 20 kV, U_2 = 35 kV, U_3 = 50 kV, U_4 = 110 kV, U_5 = 150 kV (∗) and descending order U_1 = 150 кV, U_2 = 110 кV, U_3 = 50 кV, U_4 = 35 кV, U_5 = 20 кV (×) of the measured voltage for fiber sections of equal lengths.

$$L = L_0 + \sum_{j=0}^{i-1} 2\pi\left(r_j + 2d_{31}U_j\frac{r_j}{h_j}\right)\frac{h_1}{d_f}.$$

To determine the MM with minimum error, two configurations of the measuring system were investigated, namely when higher-voltage sensors are located closer to the receiving-emitting unit (U_1 = 150 kV, U_2 = 110 kV, U_3 = 50 kV, U_4 = 35 kV, U_5 = 20 kV) and the reverse sequence (U_1 = 20 kV, ..., U_5 = 150 kV). The results of calculations by Eq. (11) for tubes made of ceramics PZT-4, PZT-5H, and PKR-73 are presented in Fig. 4. With an increase in the controlled voltage, the relative resolution capabilities of the sensors with PZT-5H and PKR-73 tubes equalize substantially over the entire range of high voltages and are in the range of 0.3–0.45%, which is preferable for practical use. In the case of PZT-4, this range is 0.8–1.2%. For comparison, the resolution capability of point fiber-optic voltage sensors based on Bragg fiber gratings reaches 2.4% [11]; when using hysteresis correction methods for piezoelectric tubes, the resolution capability is 0.5–0.75% [12], and for a voltage measuring circuit based on macrobending optical fiber, it is 0.5% [8] for voltages up to 100 V.

Conclusion. The structure of a quasi-distributed fiber-optic recirculation system for measuring high voltage using the technology of spectral multiplexing is developed. A combination of a piezoelectric ceramic tube with a wound fiber waveguide was used as the sensing element, and fiber Bragg gratings were used as spectral selective elements. The measurement principle is based on recording changes in the recirculation frequency under the influence of the applied voltage. The numerical estimates showed that for the case of a point sensor, when only one electric line is controlled, the MM relative error does not exceed 0.8% for a system with PZT-4 and 0.3% for systems with PZT-5H and PKR-73 piezoceramic tubes (tube radius 12 cm). For sensors with tubes of PZT-5H and PKR-73, the results must be further processed to minimize the effect of hysteresis. To achieve maximum resolution capability, the sensing elements should be arranged in increasing order of effective stresses in the measured lines. Moreover, depending on the radius and thickness of the tube, the length of the undeformed fiber section, the relative resolution is 0.3–0.45% for PZT-5H and PKR-73 and 0.8–1.2% for PZT-4 in the range of controlled voltages of 20–150 kV.

REFERENCES

1. F. Pan, X. Xiao, Y. Xu, and S. Ren, *Sensors*, **11**, No. 7, 6593–6602 (2011), DOI: 10.3390/s110706593.
2. A. Kumada and K. Hidaka, *IEEE Trans. Power Delivery*, **28**, No. 3, 1306–1313 (2013), DOI 10.1109/TPWRD.2013.2250315.
3. R. Han, Q. Yang, W. Sima, et al., *Electric Power Syst.Res.*, **139**, 93–100 (2016), DOI: 10.1016/j.epsr.2015.11.037.

4. K. Soobong, P. Jaehee, and H. Won-Taek, *Microw. Opt. Technol. Let.*, **51**, No. 7, 1689–1691 (2009), DOI: 10.1002/mop.24434.
5. X. Chen, S. He, D. Li, et al., *IEEE Sens. J.*, **16**, No. 2, 349–354 (2016), DOI: 10.1109/JSEN.2015.2479921.
6. G. Gagliardi and F. Marignetti, Patent EP3055703A1, subm. Aug. 17, 2016.
7. Q. Yang, Y. He, S. Sun, et al., *Rev. Sci. Instr.*, **88**, No. 10, 500–505 (2017), DOI: 10.1063/1.4986046.
8. P. Wang, Y. Semenova, Q. Wu, and G. A. Farrell, *Opt. Laser Technol.*, **43**, No. 5, 922–924 (2011), DOI: 10.1016/j.optlastec.2011.01.003.
9. A. V. Polyakov and S. I. Chubarov, "Stability of the recirculation frequency in ring structures with a fiber-optic delay line," *Izv. Vuzov. Priborostr.*, **46**. No. 5, 49–55 (2003).
10. M. A. Ksenofontov and A. V. Polyakov, "Stability of the recirculation frequency in closed regenerative-type opto-electronic systems," *Elektronika-Info*, No. 5, 76–80 (2010).
11. M. Pacheco, F. Mendoza Santoyo, A. Mendez, and L.A. Zenteno, *Meas. Sci. Technol.*, **10**, No. 9, 777–782 (1999), DOI: 10.1088/0957-0233/10/9/303.
12. G. Fusiek, P. Niewczas, L. Dziuda, and J. R. McDonald, *Opt. Eng.*, **44**, No. 11, 1–6 (2005), DOI: 10.1117/1.2124627.